Effect of Different Level Density Prescriptions on the Calculated Neutron Nuclear Reaction Cross Sections

S.B. Garg
Neutron Physics Division
Bhabha Atomic Research Centre
Trombay, Bombay 400 085, India

A B S T R A C T

A detailed investigation is carried out to determine the effect of different level density prescriptions on the computed neutron nuclear data of Ni-58 in the energy range 5-25 MeV. Calculations are performed in the framework of the multistep Hauser-Feshbach statistical theory including the Kalbach exciton model and Brink-Axel giant dipole resonance model for radiative capture. Level density prescriptions considered in this investigation are based on the original Gilbert-Cameron, improved Gilbert-Cameron, backshifted Fermi-gas and the Ignatyuk, et al. approaches. The effect of these prescriptions is discussed, with special reference to (n,p), (n,2n), (n, alpha) and total particle-production cross sections.

1. INTRODUCTION

It is well known that level density parameter plays a pivotal role in the determination of various nuclear reaction cross-sections. In this paper a detailed investigation of the four different level density prescriptions has been carried out for Ni-58 with special reference to (n,p), (n,α), (n,2n) and total production cross-sections for neutron, proton, alpha-particle and gamma-rays in the neutron energy range 5-25 MeV. The study has been performed in the framework of the multistep Hauser-Feshbach statistical model scheme /1/ which includes Kalbach exciton model /2/ and the Brink-Axel giant dipole radiation model /3/. The following four level density recipes have been examined in this investigations :

(i) Original Gilbert-Cameron Prescription /4/ (OGCP)

(ii) Improved Gilbert-Cameron Prescription /5/ (IGCP)

(iii) Back-Shifted Fermi-Gas Prescription /6/ (BSFGP) and

(iv) Prescription to include the effect of shell closures developed by Ignatyuk et al /7/ called the Ignatyuk Prescription (IP) in this write up.

2. LEVEL DENSITY FORMULATIONS

(i) Original Gilbert-Cameron Prescription

It is a two energy region representation of level densities. In the higher excitation energy region a Fermi gas level density form of the following type is used :

$$\rho_2(E,J) = \sqrt{\pi} * \exp\left[2\sqrt{aU}\right] * \rho(J) / \left(12\sigma\, a^{1/4}\, U^{5/4}\sqrt{2\pi}\right)$$

where

$$\rho(J) = (2J+1) * \exp\left[-(J+1/2)^2/2\sigma^2\right] / 2\sigma^2$$

This formula is valid for all energies greater than E_x defined by

$$U_x = 2.5 + 150/A$$

$$E_x = U_x + P(Z) + P(N)$$

Below this energy the following constant temperature formula is used :

$$\rho_1(E,J) = \exp\left[(E-E_0)/T\right] * \rho(J)/2T$$

where

a = level density parameter

σ^2 = Spin cut-off factor

$$= 0.0888 * \sqrt{aU} * A^{2/3}$$

$$a/A = 0.00917 * [S(Z) + S(N)] + C$$

C = 0.142 for spherical nuclides

= 0.120 for deformed nuclides

P(Z) and P(N) are the pairing energy corrections for protons and neutrons respectively. S(Z) and S(N) are the corresponding shell energy corrections. These parameters are taken from Cook et al /8/.

The parameters T and E_0 are determined by fitting ρ_2 and ρ_1 and their derivatives at the matching energy E_x as given below :

$$\frac{1}{T} = \sqrt{a/U_x} - \frac{3}{2U_x}$$

$$E_0 = E_x - T \log\left[T\,\rho_2(U_x)\right]$$

(ii) Improved Gilbert-Cameron Prescription

This is essentially the same as given above except that the spin cut-off factor in this formulation is given by

$$\sigma^2 = 0.146 * \sqrt{aU} * A^{2/3}.$$

(iii)Back-Shifted Fermi-Gas Prescription

Here only a single form of the level density describes the entire excitation energy region. The formula used is

$$\rho(E,J) = \exp\left[2\sqrt{aU}\right] * \rho(J) / \left(12\sqrt{2}\,\sigma\, a^{1/4} (U+t)^{5/4}\right)$$

where

$$\rho(J) = (2J+1) \exp\left[-J(J+1)/2\sigma^2\right] / 2\sigma^2$$

$$U = E - \Delta = a\,t^2 - t$$

$$\sigma^2 = 0.015 * t * A^{5/3}$$

Here t is the nuclear temperature and Δ is the energy shift. a's and Δ 's are taken from Ivascu et al /9/ for this analysis.

(iv) Ignatyuk Prescription

The formulation accounts for the energy dependence of the 'a' parameter which is brought about by the effect of shell closures. In this prescription

$$a(U) = \tilde{a}\ [1 + f(U).\ W/U\ ]$$

where $\tilde{a}$ is the asymptotic value of the Fermi gas parameter occurring at high energies and is given by

$$\tilde{a}/A = 0.1375 - 8.36 * 10^{-5} * A$$

The shell effects are included in the term δW given by

$$W = M_{exp}(Z,A) - M_{ld}(Z,A,\alpha)$$

where

M_{exp} = experimental mass of the nuclide

M_{ld} = liquid drop model based mass of the nuclide with deformation

f (U) gives the energy dependence expressed as

$$f(U) = 1 - \exp\,[-\,0.05\,U]$$

This model allows the shell effects to be included at low excitation energies while at higher energies such effects disappear.

The pairing energy corrections are again taken from Cook et al.

The level densities calculated with these four prescriptions are given in Fig.1. It may be noted that the level densities given by OGCP, IGP and IP are converging at about 5 MeV and then they start diverging with the increase in the excitation energy. Around 25 MeV IGCP and IP give level densities by factors of 2

and 6 respectively compared to that calculated with OGCP. BSFGP yields higher level density in the entire energy region by a factor of 10 compared to that given by OGCP.

3. CALCULATIONAL PROCEDURE AND DATA INPUT DETAILS

As already stated, the computations are carried out in the framework of the multistep Hauser-Feshbach data evaluation scheme. The reaction decay chain depicting the various participating nuclides considered in this investigation is shown in Fig. 2. Emissions of neutron, proton, alpha-particle and gamma-rays are included at every stage of the reaction in the equilibrium process while the emission of gamma-rays is excluded in the pre-equilibrium process.

Discrete energy levels, their spins, parities and gamma-ray branching ratios for all the nuclides depicted in Fig.2 are taken from the literature.

Transmission coefficients for neutron, proton and alpha-particles are calculated with good optical model potential parameters. For neutrons; optical model potential is that of Prince /10/, for protons; the potential is due to Mani /11/, and for alpha-particles; the potential is given by Strohmaier et al /12/. These potential parameters are listed below :

(i) Optical Model Potential Parameters For Neutrons

V (MeV) $= 49.33 - 0.48\ E + 0.0024\ E^2$

W (MeV) $= 0.0$

W_G (MeV) $= 12.0 + 3.358\ E - 0.007\ E^2$; $E < 25$ MeV

$= 0.445 + 0.908\ E - 0.011\ E^2$; $25 \leqslant E \leqslant 45$ MeV

U (MeV) $= 6.75$

r_v (fm) $= 1.2583 + 0.00258\ E$; $E < 12$ MeV

r_w (fm) $= 1.4645 - 0.0146\ E$; $E < 12$ MeV

$r_v = r_w = 1.3128 - 0.00196\ E$; $12 \leqslant E \leqslant 100$ MeV

$r_u = r_v$, $a_u = a_v = 0.7813$ fm

$a_w = 0.63$ fm.

(ii) Optical Model Potential Paramters For Protons

V (MeV) $= 41.3$; W (MeV) $= 0.9$

W_D(MeV) $= 8.2$; U (MeV) $= 7.5$

r_V (fm) $= 1.2$; r_W (fm) $= 1.25$

r_U (fm) $= 1.16$; r_C (fm) $= 1.25$

a_V (fm) $= 0.64$; a_W (fm) $= 0.56$

(iii)Optical Model Potential Parameters For Alpha-Particles

V (MeV) = 173.0 - 0.30 E

W (MeV) = 20.5 + 0.1 E

r_V (fm) = r_W (fm) = 1.445

a_V (fm) = a_W (fm) = 0.51

r_C (fm) = 1.3

The various symbols are defined below :

E = incident energy (MeV)

V = real well depth (Woods-Saxon)

W = imaginary well depth (Woods-Saxon)

W_G = imaginary well depth (Gaussian)

W_D = imaginary well depth (Derivative Woods-Saxon)

U = Spin-orbit well depth (Thomas)

r_V, r_W, r_U = radii for various potentials

r_C = radius for the Coulomb potential

a_V, a_W, a_U = diffuseness for various potentials.

(iv) Parameters for Gamma-Rays

The Brink-Axel model of giant dipole radiation has been employed to calculate the transmission coefficients for gamma-rays. For E1 radiation, the following resonance parameters due to Reffo /13/ have been used :

E1 = 16.0 MeV; Γ_1 = 3.70 MeV

E2 = 18.6 MeV; Γ_2 = 5.10 MeV

$\langle \Gamma_\gamma \rangle$ = 2200 meV; <D> = 14 keV

For M1 radiation default values of E = 8 MeV and Γ = 5 MeV are assumed.

In the pre-equilibrium description of the reaction, internal transition rates to the various exciton states are determined in terms of the average two body interaction matrix element as defined by Kalbach /14/. The exciton-state densities are calculated according to the Williams relation /15/. The K-parameter of the average reaction matrix element has been extracted as 135 MeV^3 in this analysis by matching the calculated and measured total neutron emission spectrum at 14.1 MeV as described in ref. /16/.

The computations have been performed with GNASH Code /17/.

4. CALCULATED CROSS-SECTIONS

The various computed cross-sections with the above described four level density recipes are intercompared in Figs. 3 to 8 with the OGCP case taken as the base case. A discussion of the suitability of data generated follows :

(i) (n,p) Cross-sections

The calculated (n,p) cross-sections are given in Fig.3 along with the measured data. It is noted that in the energy range extending upto 12 MeV the OGCP and IGCP yield similar results with deviations of 3% or less. The IP predictions are lower, variations being 15% or less. The data generated with BSFGP show variations ~20% or less when compared with the OGCP results.

In the energy range above 12 MeV all the four predictions fall within 15% of one-another or less. At several energy points close agreement is, however, noted between the different data sets.

The IGCP and OGCP predictions are close to the experimental values. However, in the energy range above 15 MeV all the four recipes reproduce the measured data reasonably well.

(ii) (n,α) Cross-sections

(n, α) cross-sections obtained with the four level density recipes are shown in Fig.4 together with the measured data. It is noted that in the energy range extending up to 12 MeV the data generated with BSFGP are quite low, by factors of 2 or more, when compared with the data obtained with the other three recipes which show close agreement at several energy points.

In the energy range above 12 MeV the various prescriptions yield similar cross-sections at several energy points although the maximum deviation is also seen around 30% among the different sets of data at some energy points.

The IGCP, OGCP and IP predictions are noted to be within the experimental error limits.

(iii)(n,2n) Cross-sections

The (n,2n) cross-sections are depicted in Fig.5 together with the measured data. It is noted that the IP predictions are higher throughout the entire energy range. The maximum deviation seen amongst the various sets of data is about 20% although close agreements are also noted at some energy points.

The more recent measured data of Hudson et al are represented well both in the IGCP and OGCP cases.

(iv) Total Neutron Production Cross-sections

Fig. 6 intercompares total neutron production cross-sections in the four cases. It is seen that the BSFGP case shows enhancement by 1-4% upto neutron energies of 15 MeV and above

this energy it shows depletions by about 5% compared to the OGCP case. The data is depleted by about 4% in the IGCP case whereas in the IP case it is enhanced by 1-10%.

(v) Total Hydrogen Production Cross-sections

The total hydrogen production cross-sections in the IGCP case are reduced over a wide energy range by 5-15% as shown in Fig.7. The IGCP and IP cases show marginal depletions amongst them but these two cases produce almost identical results above 12 MeV.

(vi) Total Helium Production Cross-sections

As shown in Fig.8 the total helium production cross-sections are most affected in the BSFGP case, the reduction being 40% or more. The IGCP case shows enhancement while the IP case is identical to the base OGCP case above 12 MeV.

(vii)Total Gamma-Ray Production Cross-sections

The gamma-ray production cross-section are somewhat enhanced in all cases as depicted in Fig.8 compared to the OGCP case. The IGCP and IP cases produce almost identical results.

5. CONCLUSIONS

The following conclusions are drawn from the analysis carried out in this paper :

(i) Total neutron production cross-sections in all the four level density recipes are close to one another at several energy points although a maximum deviation of about 10% is noted at some of the energy points. The (n,2n) cross-sections also exhibit a similar variation.

(ii) The (n,p) and total hydrogen production cross-sections show a maximum deviation of 20%.

(iii)The (n, α) and total helium production cross-sections are adversely affected in the BSFGP case.

(iv) The gamma-ray production cross-sections are enhanced in the BSFGP case by about 20% whereas they are comparable in other cases.

(v) The IGCP and IP cases yield almost identical results for many of the reactions investigated in this study. Since the IP case accounts for the energy dependence of the 'a' parameter, it may be adopted in the binary, tertiary and total particle production cross-sections required in reactor technology.

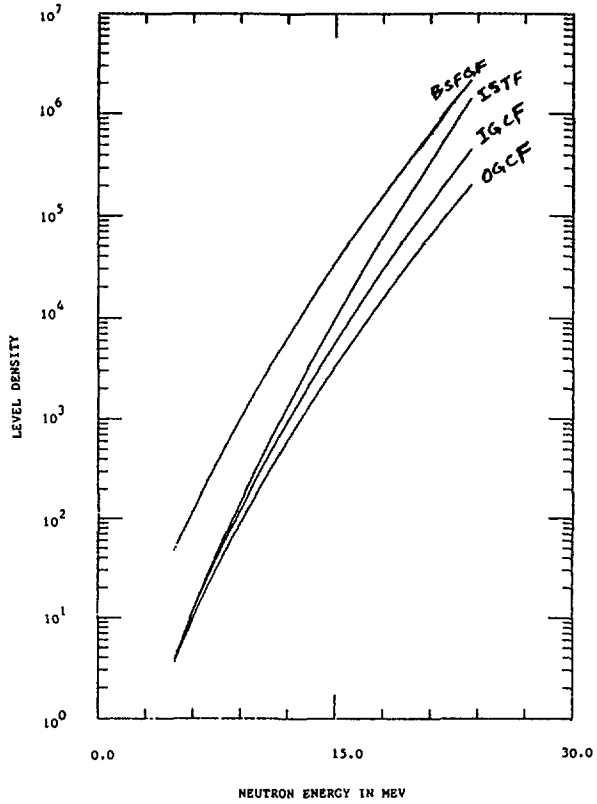

FIG. 1 LEVEL DENSITY VERSUS EXCITATION ENERGY FOR NI-58 WITH VARIOUS LEVEL DENSITY PRESCRIPTIONS

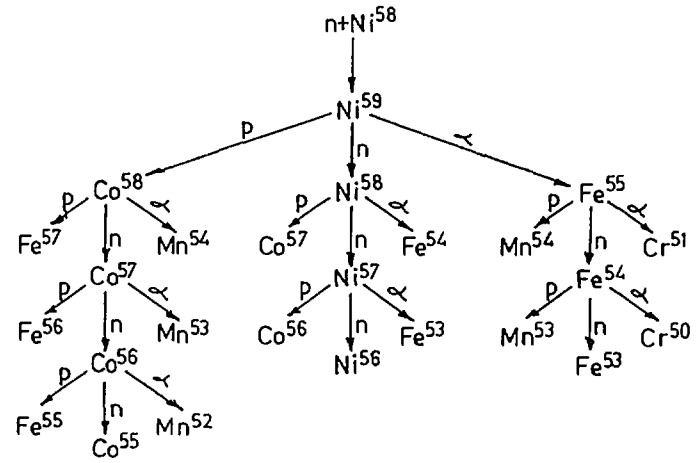

FIG.: 2 NUCLIDES PARTICIPATING IN THE DECAY CHAIN OF $n+Ni^{58}$ REACTION

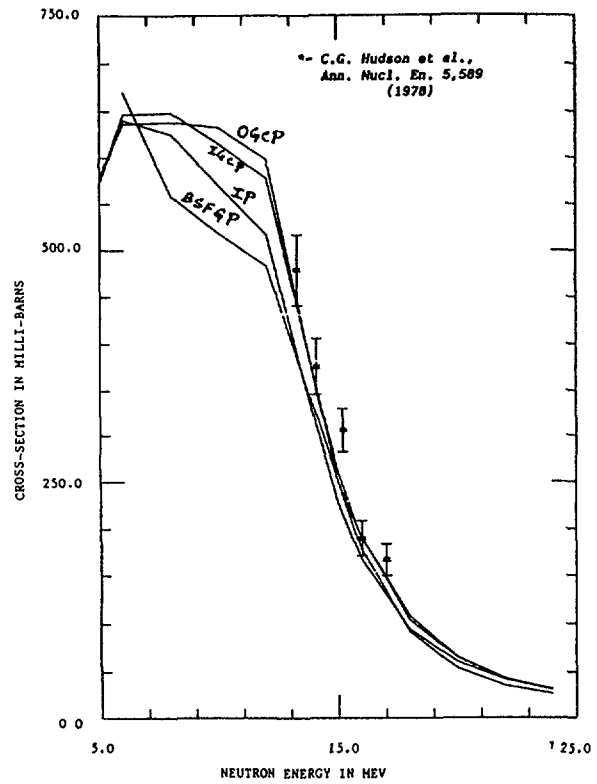

FIG. 3 INTER-COMPARISON OF (N,P) CROSS-SECTIONS OF NI-58 WITH DIFFERENT LEVEL DENSITY PRESCRIPTIONS

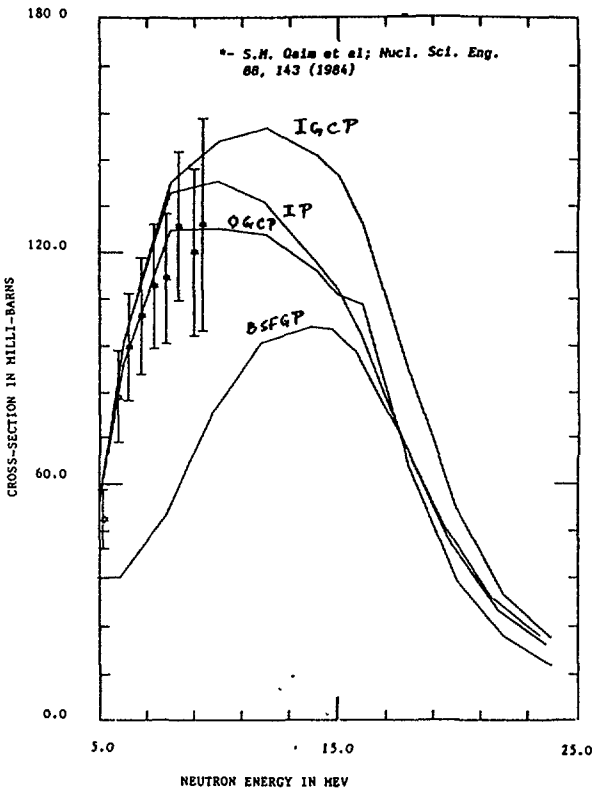

FIG 4 INTER-COMPARISON OF (N,A) CROSS-SECTIONS OF NI-58 WITH DIFFERENT LEVEL DENSITY PRESCRIPTIONS

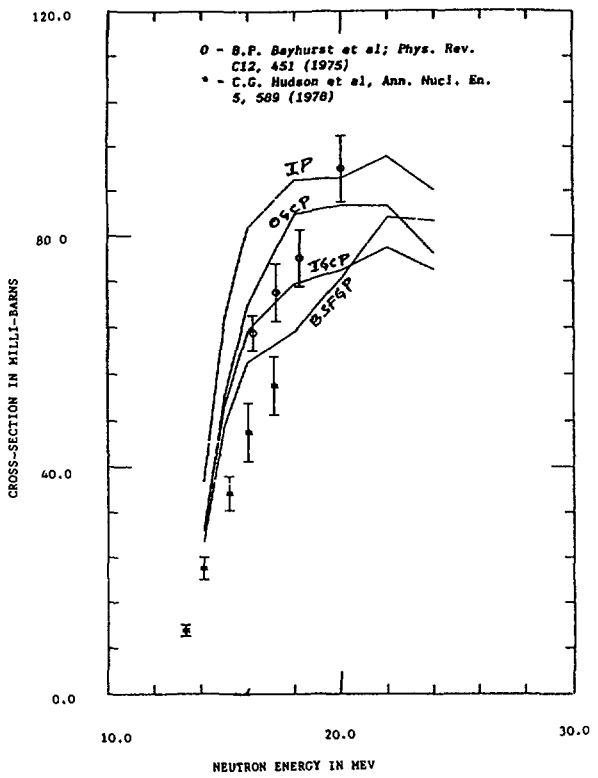

FIG. 5 INTER-COMPARISON OF (N,2N) CROSS-SECTIONS OF NI-58 WITH DIFFERENT LEVEL DENSITY PRESCRIPTIONS

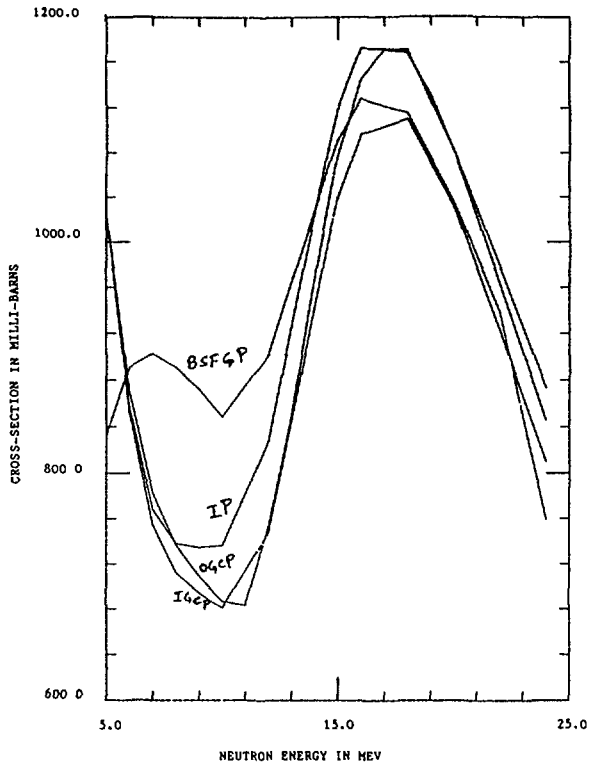

FIG. 6 INTER-COMPARISON OF TOTAL NEUTRON PRODUCTION CROSS-SECTIONS IN NI-58 WITH DIFFERENT LEVEL DENSITY PRESCRIPTIONS

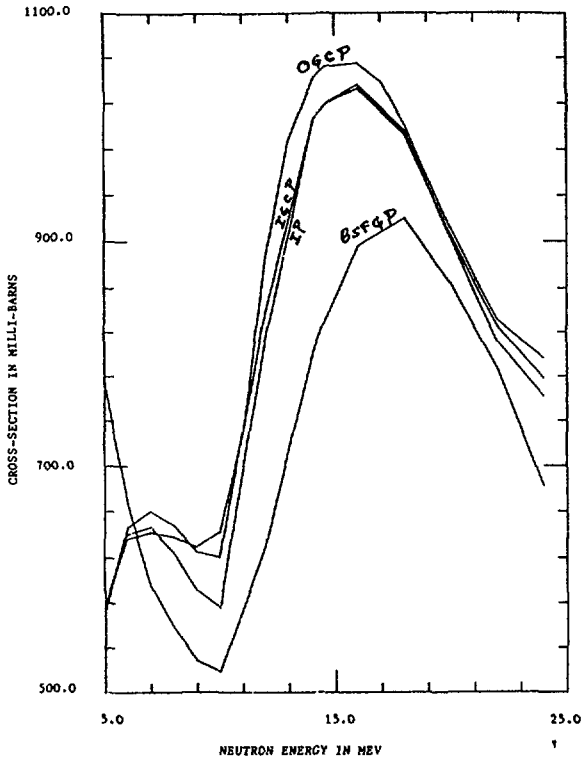

FIG. 7 INTER-COMPARISON OF TOTAL HYDROGEN PRODUCTION CROSS-SECTIONS IN NI-58 WITH DIFFERENT LEVEL DENSITY PRESCRIPTIONS

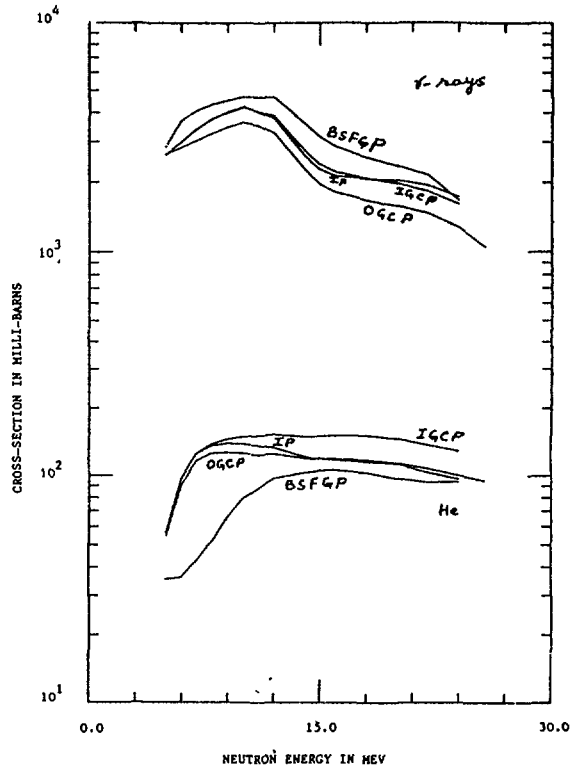

FIG. 8 TOTAL HELIUM AND GAMMA-RAY PRODUCTION CROSS-SECTIONS IN NI-58 WITH VARIOUS LEVEL DENSITY PRESCRIPTIONS

6. REFERENCES

1. W. Hauser and H. Feshbach; Phys. Rev. 87, 366 (1952)

2. C. Kalbach; Z. Phys. A283, 319 (1977)

3. D.M. Brink; Thesis, Oxford University (1955)
   P. Axel; Phys. Rev. 126, 671 (1972)

4. A. Gilbert and A.G.W. Cameron; Can. J. Phys. 43, 1446 (1965)

5. U.E. Facchini and E. Saetta-Menichla; Energ. Nucl. 15, 54 (1968)

6. W. Dilg et al; Nucl. Phys. A 217, 269 (1973)

7. A.V. Ignatyuk el al; Sov. J. Nucl. Phys. 21, 255 (1975)

8. J.L. Cook et al; Aust. J. Phys. 20, 477, (1967)

9. M. Ivascu et al; Paper Presented at the IAEA Research Co-ordination Meeting, Bologna, Italy (1986)

10. A. Prince; Nucl. Data for Science and Technology, 574 (1983)

11. G.S. Mani; Nucl. Phys. A 165, 225 (1977)

12. B. Strohmaier et al; Paper Presented at the IAEA Advisory Group Meeting on Nuclear Data for Radiation Assessment and Related Safety Aspects, Vienna (1981)

13. G. Reffo; Paper Presented at the IAEA Advisory Group Meeting on Structural Materials, Vienna (1983)

14. C. Kalbach; Z. Phys. A 287, 319 (1978)

15. F.C. Williams; Nucl. Phys. A 116, 231 (1971)

16. S.B. Garg; Investigation of Neutron Induced Reaction Cross-sections of Ni-58 and Ni-60 with Various Nuclear Model Evaluation Schemes, Paper Presented at the IAEA Research Co-ordination Meeting, Vienna (1990)

17. P.G. Young and E.D. Arthur; LA - 6947 (1977); LA-UR-88-382 (1988)